

BEAM PHASE SPACE TOMOGRAPHY FOR FXR LIA

Yuan Hui Wu[†] and Yu-Juan Chen

Lawrence Livermore National Laboratory, CA, USA

Abstract

Knowing the initial beam parameters entering an accelerator or a downstream beamline allows us to select transport tunes optimized for a desired accelerator performance. In this study, we report unfolding LLNL's FXR [1] beam parameters by using the tomography technique [2, 3] to construct the beam phase space along the accelerator's downstream beamline. The unfolded phase spaces from tomography and simulations are consistent.

INTRODUCTION

The FXR downstream system (See Fig. 1) consists of five solenoids (DR1, DR2, DR3, DR4 and DR5) and a final focusing solenoid (FF4). A diagnostic cross camera is located after DR2 to capture time resolved electron beam images. Beam emittance at the accelerator exit is needed to determine the optimal downstream tune for the desired beam spot sizes at the target for high resolution x-ray radiography. FXR can produce two 2-kA, 9-MeV beam pulses A and B. With the help of beam modelling by using AMBER PIC slice code [4], we have previously unfolded the beam energy, radius, slope and emittance at the accelerator entrance and exit (listed in Table1) on FXR by fitting the spot sizes measured through magnet scanning [5]. Figures 2 and 3 are these two pulses' experimental and simulated spot sizes vs. DR2 setting from that study.

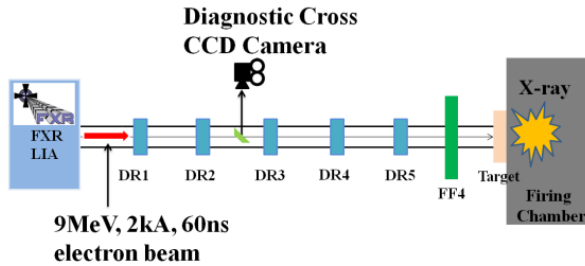


Figure 1: Schematic of FXR downstream section

Table 1: Unfolded Electron Beam Parameters at the Accelerator Exit

	Pulse A	Pulse B
Current (Ampere)	1810	1820
Energy (MeV)	8.9	8.9
Rprime (mrad)	10.2	12.9
R (mm)	6.9	7.7
Normalized emittance (mm-mrad)	1000	1050

[†] wu39@llnl.gov

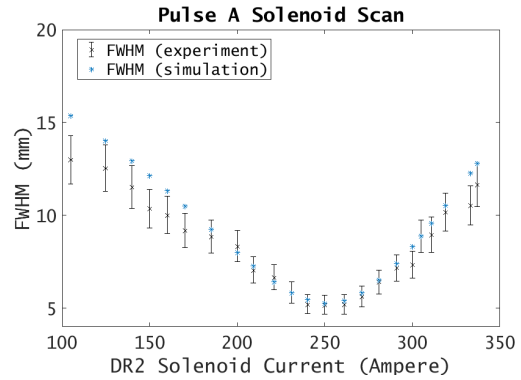


Figure 2: Pulse A spot size at the image screen varies with DR2 solenoid setting.

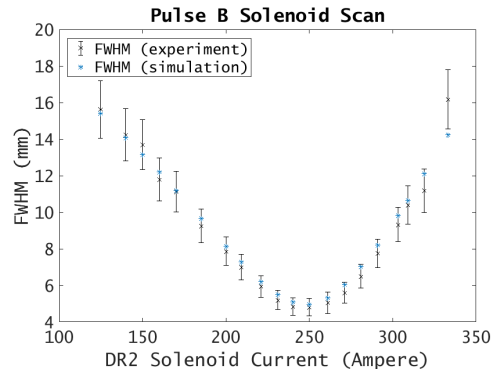


Figure 3: Pulse B spot size at the image screen varies with DR2 solenoid setting.

TOMOGRAPHY

To construct the beam phase space with the tomography technique, we have modelled the downstream lattice (shown in Fig. 4) from the accelerator exit to the diagnostic where the spot

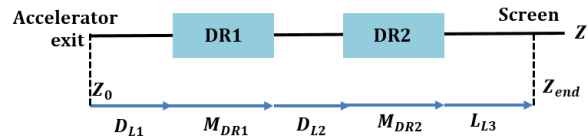


Figure 4: Schematic of FXR downstream transfer matrix from accelerator exit to the diagnostic cross.

size images are captured. The total transfer matrix M is calculated from the accelerator exit Z_0 to the image screen Z_{end} .

$$\begin{pmatrix} x_{z_1} \\ x'_{z_1} \end{pmatrix} = M \begin{pmatrix} x_{z_0} \\ x'_{z_0} \end{pmatrix}$$

$$M = D_{L3} * M_{DR2} * D_{L2} * M_{DR1} * D_{L1}$$

By knowing the total transfer matrix, we can calculate the phase space rotation angle from the accelerator exit to the image plane as $\theta = \tan^{-1} \frac{M_{12}}{M_{11}}$, and the scaling factor describing how the phase space's x or y projection at the image plane stretched by the transformation with respect to the x or y projection at the accelerator exit as $S = \sqrt{(M_{11})^2 + (M_{12})^2}$. To construct two FXR beam pulses' phase spaces using the tomography technique, we have measured their x-y configuration spaces with 84 different DR1 and DR2 settings. With these settings, their phase spaces at the image plane rotate from 0 to 180 degrees with respect to those for their nominal cases (discussed later in Phase Space and Emittance section).

BEAMS WITH SPACE CHARGES

Tomography technique has been successfully used to construct beam phase space even for extreme space charge beam [6]. The beam envelope along the lattice is needed to calculate the total transfer matrix for the space charge dominated beam. In Ref. [6], Stratakis calculated the beam sizes at different positions by solving the envelope equation with an estimated initial beam and with linear space charge forces.

We have included the space charge effects in two FXR pulses' total transfer matrices even though FXR beams are not space-charge dominated in the downstream beamline. We used the unfolded beam parameters in Table 1 for Tomography technique's initial beam parameters. Instead of solving the envelope equation as in Ref. [6], each beam pulse's radius $r(z)$ is obtained from AMBER PIC slice simulations. As expected, the differences between the calculated transfer matrices with and without space charge terms for FXR's two beam pulses are small. The differences in the scaling factors and the rotation angles are less than 6%.

PHASE SPACE AND EMITTANCE

The nominal DR1 and DR2 current is 208 A and 191 A, respectively. Let the nominal total transfer matrix for this setting be M_{nominal} . The net transfer matrix M_{net} between the nominal phase space and the other setting's phase space is

$$M_{\text{net}} = M * M_{\text{nominal}}^{-1}$$

Applying M_{net}^{-1} to another setting's phase space parameters would convert it to the nominal phase space parameters (see Fig. 5)

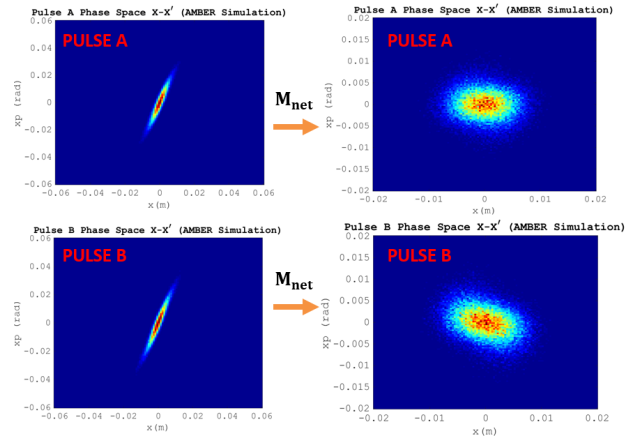


Figure 5: Demonstration of Pulses A's and B's beam phase spaces for DR1 = 208 A and DR2 = 300 A (at the left) transferred to their nominal beam phase spaces (at the right) via the inverse of their net transfer matrices.

Figure 6 shows Pulses A's and B's beam phase spaces at the image screen. The phase spaces obtained from AMBER simulations alone is given at the left. The phase spaces constructed from tomography technique based on the simulated x-y configurations at the image screen is given in the middle. The phase spaces constructed from tomography technique based on the experimental x-y configurations at the image screen are presented at the right. The phase spaces obtained through these three methods are very similar. Based on the reconstructed phase spaces' intensity output and using

$$\epsilon_x = 4\beta\gamma\sqrt{\langle x^2 \rangle \langle x'^2 \rangle - \langle xx' \rangle^2}$$

two pulses' normalized emittances are given in Table 2.

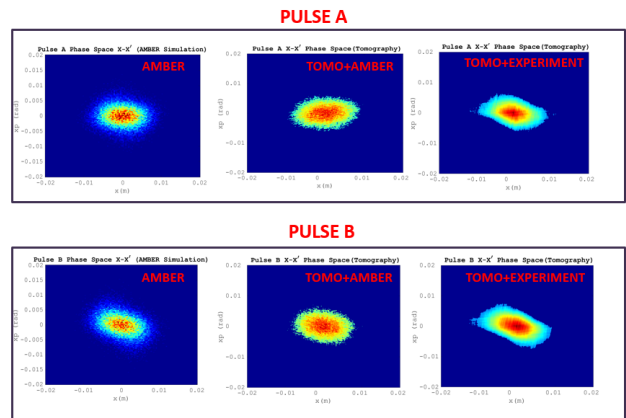


Figure 6: Beam phase spaces at the image screen obtained from AMBER simulation (left), constructed by using tomography technique based on simulated image screen data (middle) and based on the experimental image screen data (right).

Table 2: Calculated Emittances Based on Reconstructed Beam Phase Spaces

	Pulse A	Pulse B
Normalized emittance (mm-mrad), include linear space charge	946±254	1080±215
Normalized emittance (mm-mrad), not include linear space charge	933±167	1066±234

[5] Y. H. Wu, et. al, “Unfolding electron beam parameters using magnet scan”, LLNL-conf-704030, NAPAC, CHICAGO, 2016. Page 1-3.
 [6] D. Stratakis, PhD dissertation UMD 2008, Chapter 5.1.2.

SUMMARY AND FUTURE STUDY

We have performed a beam space tomography technique to measure two beam pulses’ emittances on FXR linear induction radiography accelerator. The reconstructed beam phase spaces are similar with what we obtain from AMBER PIC simulations. Hence, the calculated emittances through tomography are consistent with the predicted values from AMBER simulations.

The 2-kA, 9-MeV beams used in this tomography technique study are not space charge dominated. To achieve the best tomography image, it generally requires rotating the object’s phase space from 0 to 180 degree with linear optics first and then taking the object’s projected images. To measure the beam emittance with the tomography technique, we need to vary the transport magnets’ setting to achieve 0-180 degree phase space rotation. For a space charge dominated beam, varying transport magnet settings widely for large phase space rotation usually can either lead to uncontrolled beam expansion or strong beam radius pinching. Both can potentially cause emittance growth. We plan to study the limitation of this technique by extending this study to a space charge dominated beams.

ACKNOWLEDGEMENTS

The authors would like to thank Jennifer Ellsworth, Blake Kreitzer and Jan Zentler for their assistance in performing the experiments. This work was performed under the auspices of the U.S. Department of Energy by Lawrence Livermore National Laboratory under Contract DE-AC52-07NA27344.

REFERENCES

[1] L. G. Multhaupt, UCRL-JC-148534, *Proceedings, 25th Conference on High Speed Photography and Photonics*, 2002, page 1-12.
 [2] D. Stratakis, et. al, Generalized phase-space tomography for intense beams, *PHYSICS OF PLASMAS* 17, 056701 (2010), page 1-6.
 [3] Dao Xiang, et. al, Transverse phase space tomography using a solenoid applied to a thermal emittance measurement, *PRST 12*, 022801 (2009), page 1-7.
 [4] J. L. Vay and W. Fawley, Amber user’s Manual. http://www.iaea.org/inis/collection/NCLCollectionStore/_Public/32/069/32069294.pdf?r=1